Sum-Rate Maximization of IRS-Aided SCMA System

Saumya Chaturvedi, Vivek Ashok Bohara, Zilong Liu, Anand Srivastava

***Abstract*—We study an intelligent reflecting surface (IRS)-aided downlink sparse code multiple access (SCMA) system for massive connectivity in future machine-type communication networks. Our objective is to maximize the system sum-rate subject to the constraint of minimum user data rate, the total power of base station, SCMA codebook structure, and IRS channel coefficients. To this end, a joint optimization problem involving IRS phase vector, factor graph matrix assignment, and power allocation problem is formulated, which is non-convex in nature. This problem is solved by developing an alternating optimization (AO) algorithm. A key idea is to first divide the formulated non-convex problem into three subproblems (i.e., factor graph matrix assignment, power allocation, and phase vector of IRS) and then tackle them iteratively. The validity of the proposed schemes is shown using the simulation results. Moreover, compared to the SCMA system without IRS, a significant performance improvement in the IRS-aided SCMA system is shown in terms of achievable sum-rate.**

***Index Terms*—Factor Graph Matrix Assignment, Intelligent Reflecting Surface (IRS), Power Allocation, Phase Shifts Optimization, Sparse Code Multiple Access (SCMA).**

I. Introduction

Recently, intelligent reflecting surfaces (IRSs) have attracted tremendous research attention owing to their potential of supporting intelligent and more efficient wireless communications [1], [2]. An IRS is a planar array made up of number of low cost intelligently controllable passive elements. These elements can passively reflect the incoming signals by smartly changing their amplitude and phase, etc. Thus, IRSs are capable of overcoming the problem of signal blockage in wireless systems, thus enabling a controllable and more reliable wireless propagation [2].

At the same time, it is evident from the literature that non-orthogonal multiple access (NOMA) technique improves spectral efficiency by supporting massive connectivity [3], [4]. The primary objective of NOMA is to provide overloaded multiuser communications (thus higher spectrum efficiency) which are concurrently carried out over the same resource elements (REs) using different power levels or codebooks (CBs). In general, there are mainly two types of NOMA schemes: code-domain NOMA (CD-NOMA) and power-domain NOMA (PD-NOMA). In PD-NOMA, number of users communicate over the same REs by assigning them with different power levels [5], [6]. In contrast, CD-NOMA may be regarded as an extension of CDMA where different users are allocated with distinctive CBs or sequences. One of the major CD-NOMA techniques, called sparse code multiple access (SCMA) was proposed in 2013 [7]. Compared to the orthogonal multiple access (OMA) schemes, SCMA can serve more number of users and can thus improve the system capacity significantly. Also, SCMA outperforms PD-NOMA in terms of both sum-rate [8] and bit error performance (BER) [9], [10], but at the cost of higher system complexity. Motivated by this, several low complexity detectors have been developed for SCMA systems [11]. SCMA employs a multi-dimensional CB which leads to a constellation shaping gain and consequently better spectral efficiency when compared to other CD-NOMA schemes as low density spreading code division multiple access (LDS-CDMA) and low density signature-orthogonal frequency division multiplexing (LDS-OFDM) [7]. SCMA has been studied for various applications, such as grant-free transmission, visible light communication, high mobility communication, etc [12]–[15].

A. Related Works

This paper investigates the integration of IRS with NOMA schemes which is an efficient way to enlarge the network coverage and boost the spectrum efficiency. Several research works incorporating NOMA with IRS systems have been presented in the literature [16]–[27]. In [16], the sum-rate was maximized in an IRS-aided NOMA system by jointly optimizing the IRS phases and beamforming at the base station (BS). In [17], the rate regions calculated for both OMA and NOMA techniques are characterized by the IRS reflection matrix. In [18], [19], the objective was to minimize the total transmit power by optimizing the active and passive beamforming. In [20], the required minimum transmit power was analyzed between NOMA and OMA schemes in the IRS-assisted system. The minimum signal-to-interference-plus-noise-ratio (SINR) was maximized in [21] by phase optimization and transmit power allocation, in case of single and multi-antenna scenario. [22] investigated the power allocation, channel assignment, and IRS reflection matrix to maximize the system throughput. In [23], the weighted sum-rate was maximized by optimizing the deployment of the IRS location, power allocation, and the reflection matrix in

Saumya Chaturvedi, Vivek Ashok Bohara, and Anand Srivastava are with Indraprastha Institute of Information Technology (IIIT-Delhi), Delhi, New Delhi, 110020, India (e-mail: {saumyac, vivek.b, anand}@iiitd.ac.in). Zilong Liu is with the School of Computer Science and Electrical Engineering, University of Essex, Colchester CO4 3SQ, U.K. (e-mail: zilong.liu@essex.ac.uk).

a NOMA system. [24] proposed a resource allocation framework for maximizing the sum-rate through optimized decoding order, user association, power allocation, and reflection matrix. The idea of integrating the multiple-input–multiple-output (MIMO) and NOMA with IRS was mentioned in [25], where the performance gains and challenges of the MIMO-NOMA with IRS were discussed. In [27], the power minimization problem was investigated for IRS-empowered multi-group coordinated multi-point-NOMA networks with error propagation.

It is noted that most of the above works were mainly focused on the integration of PD-NOMA with IRS. In contrast to the existing studies, this work focuses on the integration of IRS with SCMA. A major feature of SCMA is to take advantage of sparse CBs to permit simultaneous multiuser communication [7], [28]. An IRS-aided SCMA system was firstly investigated in [29], in which a low-complexity decoder was proposed. [30] analyzed the symbol error rate, diversity order, and the sum-rate in an IRS-aided SCMA system. [31] maximized the received signal-to-noise-ratio (SNR) by optimizing the IRS coefficients.

B. Contributions

Motivated by the advantages of both SCMA and IRSs, the IRS-aided SCMA system can be a promising candidate to improve the sum-rate for the next generation machine-centric communication networks. The proposed system model consists of an IRS-aided SCMA system in which users are in non-line-of-sight (NLoS) with the base station (BS) and thus are served using IRS. The aim is to maximize the sum-rate of this system considering the constraints of IRS, BS, and SCMA. However, the formulated optimization problem is non-convex which is hard to solve. This is because the optimization problem is a combination of different optimization variables, such as the phase vector of IRS, transmit power and factor graph matrix variables. Thus, enhanced algorithms are needed to optimize the IRS-assisted SCMA systems. Further, it is important to consider both channel state information (CSI) and fairness parameters in the optimization problem, as each user experiences different channel fading. So far, few works have investigated IRS-aided SCMA systems [29]–[31]. A satisfactory solution to the sum-rate optimization problem considering the multi-user interference in the IRS-aided SCMA system is not known, to the best of our knowledge. In this work, our aim is to maximize the sum-rate in a downlink IRS-aided SCMA system by optimizing the factor graph matrix, power allocation, IRS reflection matrix, and choose the appropriate IRS deployment. In Table I, we summarize the unique contributions of this work compared to [29]–[31].

The main contributions of this work are summarized as follows:

- A downlink IRS-aided SCMA is proposed for sum-rate enhancement. For the proposed system, a sum-rate maximization problem is formulated, subject to the SCMA CB structure, QoS requirements, and IRS reflecting elements constraints. In order to do so, the transmit power, factor graph matrix, and IRS reflection matrix are optimized. We show that the formulated optimization problem is a mixed-integer non-linear programming (MINLP) problem, which is non-convex.
- To tackle the formulated optimization problem, an alternating optimization (AO) based iterative algorithm is proposed. The fundamental idea is to divide the main optimization problem into three subproblems which are then solved iteratively. Firstly, we work on the factor graph matrix assignment sub-problem using the effective channel gains. We then use Lagrange dual decomposition method for power allocation. Finally, the phase optimization problem is solved subject to IRS reflecting elements constraints using the Riemannian conjugate gradient (RCG) algorithm.
- After optimizing the factor graph matrix assignment, power allocation, and the phase vector of the IRS, the performance of the proposed algorithm is evaluated for IRS-aided SCMA system. Further the simulation results show that the proposed IRS-aided SCMA system improves the sum-rate performance significantly when compared to an SCMA system without IRS.

It is noted that the AO based algorithms have been previously employed in a number of works in wireless communication as well as in IRS-assisted communication networks [31]–[35]. However, for every work, the formulated problem is unique and so is the application of the AO algorithm and the optimization of the variables. SCMA is different from other multiple access schemes and generally shows better performance when compared with other schemes in terms of sum-rate, BER, and access delay [8]–[10]. Consequently, the problem formulation is different from the prior works discussed in the literature on IRS and SCMA [29]–[31]. In the proposed work, the fundamental idea is to segregate the main optimization problem into three subproblems which are then solved iteratively. Also, there are different ways to maintain the fairness among users [36]–[38]. In our work, the fairness among users is maintained in terms of data rate as employed in [39], and power allocation is done from total power budget. Through the proposed work, it has

TABLE I
A COMPARISON OF CONTRIBUTIONS WITH EXISTING WORKS ON IRS-ASSISTED SCMA SYSTEM [29]–[31]

Work	Main Contribution
[29]	First work on uplink IRS-aided SCMA system, proposed a low-complexity decoder.
[30]	The diversity orders are derived for random and coherent phase shifts in uplink IRS-aided SCMA system.
[31]	Optimized the IRS phase vector to improve the received SNR in an uplink IRS-aided SCMA system.
Proposed work	Formulate a sum-rate maximization problem in downlink IRS-aided SCMA system considering the multi-user interference and optimize the the power allocation, IRS reflection matrix and factor graph matrix assignment.

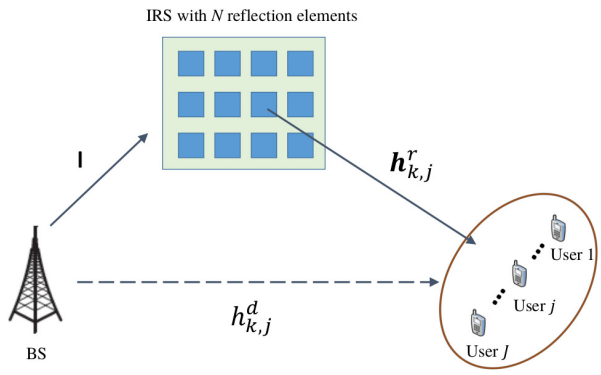

Fig. 1. The system model of an IRS-aided SCMA system with J users.

also been shown that the power and factor graph matrix assignment plays a significant role in maximizing the sum-rate of the IRS-aided SCMA system. Moreover, for a good deployment location with optimized phase shifts of IRS, the power required to provide certain sum-rate is less compared to a location with random phase shifts.

The paper outline is as follows. Section II discusses the IRS-aided SCMA system model and formulated problem. In Section III, we discuss the proposed algorithms for the factor graph matrix assignment, power allocation, and IRS phase optimization. The results are presented and analyzed in Section IV. The paper is concluded in Section V.

We represent a scalar, vector, and matrix by x, $\mathbf{x}$, $\mathbf{X}$, and conjugate transpose of $\mathbf{X}$ is represented by $\mathbf{X}^H$, respectively. We use notations $\mathbb{B}$, $\mathbb{R}$, and $\mathbb{C}$ to represent the set of binary, real, and complex numbers, respectively. 'log($\mathbf{x}$)' represents the natural logarithm of $\mathbf{x}$ and diag($\mathbf{x}$) denotes the diagonal matrix. $x \in \mathcal{CN}(\mu, \sigma^2)$ denotes that x is a circularly complex Gaussian random variable (RV) with mean μ and variance σ^2. The composition of functions f_1 and f_2 over the variable x is given as $(f_1 \circ f_2)(x) = f_1(f_2(x))$. x^* denotes the complex conjugate, $|x|$ denotes the absolute value, and Re$\{x\}$ denotes the real part of a complex number x. Tr($\mathbf{X}$) denotes the trace of the square matrix $\mathbf{X}$.

II. System Model and Problem Formulation

A. System Model

As shown in Fig. 1, a downlink ($K \times J$) IRS-aided SCMA system is considered, which consists of a BS, J single-antenna users communicating over K REs and an IRS equipped with N reflection elements. To support massive connectivity, in the SCMA system, the number of users being served is larger than the number of resource nodes (RNs), i.e., $J > K$. Each user is given a CB of size $K \times M$, where M is the number of K-dimension codewords in the CB. Such a CB may be denoted by $\mathcal{X}_j, \forall j \in J$, and each CB satisfies Tr$(\mathcal{X}_j \mathcal{X}_j^H) = M$. The SCMA encoder selects a column of $\mathcal{X}_j$ for user j, corresponding to the input message $\mathbf{b}_j$.

Practically, the IRS is managed by an intelligent controller connected to the BS. The IRS-assisted link suffers from "double fading" effect [40], [41]. Let $\Theta = \text{diag}(\boldsymbol{\theta}) \in \mathbb{C}^{N \times N}$ denote the IRS reflection coefficients matrix with $\boldsymbol{\theta} = [\theta_1, \theta_2, \cdots, \theta_N]$ and $\theta_n = \exp^{j\phi_n}$, where $\phi_n \in [0, 2\pi)$ denotes the reflection phase shift of the nth IRS reflecting element. The baseband equivalent channels at RE k between BS and user j, between IRS and user j at RE k, and between BS and IRS are denoted by $h^d_{k,j} \in \mathbb{C}^{1\times 1}$, $\mathbf{h}^r_{k,j} \in \mathbb{C}^{N\times 1}$, and $\mathbf{l} \in \mathbb{C}^{1\times N}$ respectively. All the channel fading vectors are assumed to be independent complex Gaussian random variables. It is assumed that all the required CSI is available at the BS. The signal received at RE k is [7]

$$\begin{aligned} y_k &= \sum_{j=1}^{J} h^d_{k,j} f_{k,j} x_{k,j} + \sum_{j=1}^{J} (\mathbf{l}\Theta\mathbf{h}^r_{k,j}) f_{k,j} x_{k,j} + n_k, \\ &= \sum_{j=1}^{J} (h^d_{k,j} + \mathbf{l}\Theta\mathbf{h}^r_{k,j}) f_{k,j} x_{k,j} + n_k, \end{aligned} \tag{1}$$

where $x_{k,j}$ denotes the codeword element of the jth user on kth RE, $f_{k,j} = 1$ indicates that user j has active power transmission over RN k (otherwise, no power transmission), and $n_k \sim \mathcal{CN}(\mathbf{0}, \sigma^2)$ denotes the additive white Gaussian noise (AWGN) at the kth RE. The jth user considers the signals from all the other users (i.e., $x_{k,1}, \cdots, x_{k,j-1}, x_{k,j+1}, \cdots, x_{k,J}$) as interference on the k RE. Thus, the decoding SINR of $x_{k,j}$ at RE k and user j is given as:

$$\gamma_{k,j} = \frac{|(h^d_{k,j} + \mathbf{l}\Theta\mathbf{h}^r_{k,j})|^2 E(x^2_{k,j})}{\sum\limits_{\substack{i\in S_k \\ i\neq j}} |(h^d_{k,i} + \mathbf{l}\Theta\mathbf{h}^r_{k,i})|^2 E(x^2_{k,i}) + \sigma^2}, \tag{2}$$

where S_k denotes the set of users communicating at the k RE.

B. Introduction to SCMA

SCMA is mainly characterized by the sparse CBs, and the RE-user association in the SCMA can be represented bipartite factor graph. In this article, we consider a regular factor graph, where each user node (UN) has d_v number of neighboring RNs, and each RN has d_f number of neighboring UNs. Fig. 2 shows the user-RE association with a factor graph, where the circle represents the UN and the box represents RN. It is to be noted that the first RN is connected to the second, third, and fifth UN. This means that data of second, third, and fifth users is being transmitted on the first RE.

An alternative way of representing the association between UNs and RNs is by a factor graph matrix, $\mathbf{F}$ [7]. Let $\mathbf{F} \in \mathbb{B}^{K\times J}$ be the factor graph matrix with each element $f_{k,j}$. The factor graph matrix corresponding to Fig. 2 is given as

$$\mathbf{F}_{4\times 6} = \begin{bmatrix} 0 & 1 & 1 & 0 & 1 & 0 \\ 1 & 0 & 1 & 0 & 0 & 1 \\ 0 & 1 & 0 & 1 & 0 & 1 \\ 1 & 0 & 0 & 1 & 1 & 0 \end{bmatrix}. \tag{3}$$

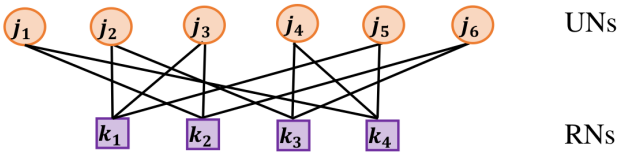

Fig. 2. The factor graph corresponding to (3) with $d_v = 2$ and $d_f = 3$.

Next, Maximum a-posteriori (MAP) can be used to detect the SCMA multi-user codeword $\mathbf{X} = [\mathbf{x}_1, \mathbf{x}_2, \cdots, \mathbf{x}_J]$ as [42], [43]

$$\hat{\mathbf{X}} = \underset{\mathbf{x}_j \in \mathcal{X}_j, \forall j}{\operatorname{argmax}} p(\mathbf{X}|\mathbf{y}) \,. \tag{4}$$

The marginal distribution of (4) with respect to $\mathbf{x}_j$ leads to the detected symbol of the jth user. Next, using Bayes' rule, the detected codeword of jth user is:

$$\hat{\mathbf{x}}_j = \underset{\mathbf{x}_j \in \mathcal{X}_j}{\operatorname{argmax}} \sum_{\sim \mathbf{x}_j} \left(P(\mathbf{X}) \prod_{k=1}^{K} f(y_k|\mathbf{X}) \right) , \quad \text{for } j = 1, \cdots, J. \tag{5}$$

where $f(y_k|\mathbf{X})$ denotes the conditional probability density function (PDF) of the received value, and $P(\mathbf{X})$ represents the joint a-priori probability mass function (PMF). Solving the problem in (5) with brute force leads to exponential complexity. The above problem can be solved using an iterative message passing algorithm (MPA) with lower complexity [42], [44]. The complexity of SCMA multi-user detection using MPA is proportional to M^{d_f}.

C. Problem Formulation

The goal is the maximization of the sum-rate by jointly optimizing the factor graph matrix, transmit power allocation, and the reflection matrix at IRS, taking into account the constraints of transmit power, minimum data requirement of the users, IRS constraints, and SCMA CB structure. The power allocation matrix can be expressed as $\mathbf{P} = (p_{k,j})_{K \times J}$, where the power allocated to user j on RE k is $p_{k,j}$. Also, we believe that choosing the factor graph matrix based on the system scenario improves the performance. Mathematically, the formulated sum-rate optimization problem is given as:

$$\mathcal{P}(\mathrm{A}): \quad \max_{\mathbf{F},\mathbf{P},\boldsymbol{\theta}} f_{\mathrm{A}}(\mathbf{F},\mathbf{P},\boldsymbol{\theta}) = \sum_{k=1}^{K}\sum_{j=1}^{J} \log_2(1+\gamma_{k,j}) \tag{6a}$$

$$\text{s.t.} \quad |\theta_n| = 1, \ \forall\ n \in [1, N], \tag{6b}$$

$$\sum_{k=1}^{K}\sum_{j=1}^{J} f_{k,j} p_{k,j} \leq \mathrm{P}_{\mathrm{tot}}, \tag{6c}$$

$$\sum_{k=1}^{K} \log_2(1+\gamma_{k,j}) \geq \mathrm{R}_{\mathrm{min}}, \tag{6d}$$

$$p_{k,j} \geq 0, \quad \forall\ 1 \leq k \leq K, 1 \leq j \leq J, \tag{6e}$$

$$\sum_{j=1}^{J} f_{k,j} \leq d_f, \quad \forall\ k \in K, \tag{6f}$$

$$\sum_{k=1}^{K} f_{k,j} \leq d_v, \quad \forall\ j \in J, \tag{6g}$$

$$\mathbf{F}_j \neq \mathbf{F}_{j'}, \quad \forall\ j \neq j' \in J, \tag{6h}$$

$$f_{k,j} \in \{0,1\}, \ \forall\ 1 \leq k \leq K, 1 \leq j \leq J, \tag{6i}$$

where $\gamma_{k,j}$ is as defined in (2), $\mathrm{P}_{\mathrm{tot}}$ denotes the total transmit power at the BS, $\mathrm{R}_{\mathrm{min}}$ is the minimum rate requirement of the user. Constraint (6b) represents the unit modulus constraint for the IRS reflection coefficient, constraint (6c) is the total transmit power constraint of BS and constraint (6d) guarantees the rate fairness among all users. Constraint (6f) limits the maximum number of signals multiplexed on each RE, constraint (6g) denotes a codeword has maximum d_v number of non-zero values, and constraint (6h) denotes that no two columns of the factor graph matrix are same, and constraint (6i) denotes that each element of the factor graph matrix is either zero or one.

The optimization problem in $\mathcal{P}(\mathrm{A})$ is a highly-coupled non-convex problem, making it hard to find the global optimal solution [45]. Next, we propose the AO based algorithms to find an efficient suboptimal solution.

III. Alternating Optimization

The main idea of the AO approach is to divide the optimization problem into several subproblems and are alternately optimized. Each subproblem is solved under some constraints, while other subproblems remain at their last updated values [34], [46], [47]. In our case, we divide the problem in (6) into three subproblems, i.e., factor graph matrix assignment, power optimization, and the IRS phase optimization, and solve using AO based algorithm. Firstly, an algorithm based on the channel gain of REs is proposed for solving the factor graph matrix assignment subproblem. Next, the power allocation subproblem is solved using a low complexity Lagrange dual decomposition method. Finally, we use the RCG algorithm to optimize the IRS phase shifts. Our proposed approach is shown in a flow chart in Fig. 3.

A. Factor graph matrix assignment

For a given power $\mathbf{P}$, and phase vector $\boldsymbol{\theta}$, (6) is given as:

$$\mathcal{P}(\mathrm{A1}): \quad \max_{\mathbf{F}} f_{\mathrm{A1}}(\mathbf{F}) = \sum_{k=1}^{K}\sum_{j=1}^{J} \log_2(1+\gamma_{k,j}) \tag{7a}$$

$$\text{s.t.} \quad (6\mathrm{f}), (6\mathrm{g}), (6\mathrm{h}), (6\mathrm{i}). \tag{7b}$$

To solve the factor graph matrix assignment subproblem $\mathcal{P}(\mathrm{A1})$ in (7), a low complexity algorithm is proposed. The proposed algorithm makes use of the instantaneous channel gains or CSI.

Algorithm 1: The Factor graph matrix assignment algorithm

Inputs:
J: Number of users.
K: Number of REs.
d_f: Degree of each RN.
d_v: Degree of each UN.
$\mathbf{H}_{\text{tot}}$: Overall channel gain matrix of size $K \times J$ from direct and IRS-assisted path.
Output:
$\mathbf{F}$: Binary Factor graph matrix.
Initialize:
Initialize $\mathbf{F}_{\text{ini}}$ with all values equal to one, and $\mathbf{F}$ with all values equal to zero.

```
Calculate the SINR S = (γ_{k,j}) forall 1 ≤ k ≤ K, 1 ≤ j ≤ J.
Calculate the average RMS value, r of S along first dimension for each user .
Sort r in the descending order.
for i = 1 : J do
    For the S column with index r(i), find the d_v largest values.
    For the d_v largest values chosen in step 5, set their corresponding indices in F equal to one.
    if F_i ≠ F_j or Σ_{j=1}^{J} F_{k,j} ≤ d_f, ∀ k ∈ K then
        Set the largest value of S in the column with index r(i) equal to zero.
        Go to Step 5, and choose the index of next d_v largest values.
    end if
end for
```

The objective of **Algorithm 1** is to design $\mathbf{F}$ by taking advantage of the channel information. In this algorithm, initially, we consider a factor graph matrix with all values equal to one and calculate the SINR as shown in (2) for each $1 \leq k \leq K, 1 \leq j \leq J$. The SINR matrix is given as $\mathbf{S} = (\gamma_{k,j})_{K \times J}$. Then, the root mean square (RMS) of all the users is calculated and sorted in the descending order. Starting with the user with the highest RMS value, we select d_v number of REs with the highest SINR among all available REs and then assign those to the corresponding user. The sparsity of the resultant factor graph is maintained by selecting only d_v number of REs in each step. We then repeat the similar procedure for the next highest RMS value user until all the users are assigned to the corresponding REs, considering the constraints shown in (6f, 6g, 6h).

B. Power Allocation

Given phase vector of the IRS $\boldsymbol{\theta}$ and $\mathbf{F}$, (6) is given as:

$$\mathcal{P}(\text{A2}): \quad \max_{\mathbf{P}} f_{\text{A2}}(\mathbf{P}) = \sum_{k=1}^{K}\sum_{j=1}^{J} \log_2(1+\gamma_{k,j}) \tag{8a}$$

$$\text{s.t.} \quad (6c), (6d), (6e). \tag{8b}$$

With given $\boldsymbol{\theta}$, the channel gain between BS to IRS, IRS to users, and BS to users becomes fixed. This simplifies the given optimization problem in (8), but it still remains to be a non-convex problem [39]. The Lagrange dual decomposition method is used to find a near-optimal solution for the

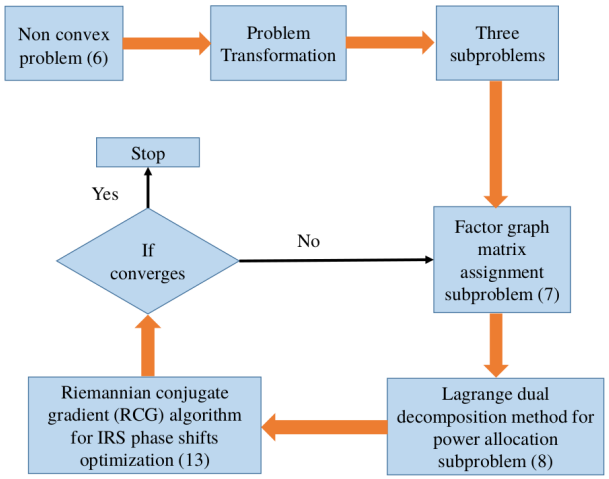

Fig. 3. The flow chart of the proposed AO-based method for solving problem (6).

subproblem (8). The Lagrangian of (8) is given as

$$L(\{\mathbf{P}\}, \boldsymbol{\lambda}, \mu) = \sum_{j=1}^{J}\left[(1+\lambda_j)\sum_{k=1}^{K}\log_2(1+\gamma_{k,j}) - \lambda_j \mathrm{R}_{\min}\right] + \mu\left(\mathrm{P}_{\text{tot}} - \sum_{k=1}^{K}\sum_{j=1}^{J} p_{k,j}\right), \tag{9}$$

where $\boldsymbol{\lambda} = \{\lambda_1, \cdots, \lambda_J\}, \lambda_j$ and μ are the Lagrange dual variables of user j. The dual problem in (9) is called the unconstrained maximization of the Lagrangian function. Thus, dual objective is $\mathcal{G}(\boldsymbol{\lambda}, \mu) = \max_{\{\mathbf{P}\}} L(\{\mathbf{P}\}, \boldsymbol{\lambda}, \mu)$, and the dual problem is given as

$$\min_{\boldsymbol{\lambda}, \mu} \mathcal{G}(\boldsymbol{\lambda}, \mu) \tag{10a}$$

$$\text{s.t.} \quad \boldsymbol{\lambda}, \mu \succcurlyeq 0 \tag{10b}$$

Applying the KKT conditions [48] on (10), the next step is to differentiate the Lagrangian in (9) with respect to $p_{k,j}$ and then the result is made equal to zero. Next, we get the following expression

$$\frac{(1+\lambda_j)\ g_{k,j}}{\ln(2).(1+\sum_{i\in S_k} p_{k,i}\ g_{k,i})} + \text{ negative terms} = \mu, \tag{11}$$

where $g_{k,j}$ is the normalized channel gain at user j and RE k. The negative terms arise because of the multi-user interference, which can be efficiently eliminated by designing CB wisely, and thus, the negative terms in (11) become negligible. The power allocated to user j at RE k can be expressed as

$$\hat{p}_{k,j} = \left[\frac{(1+\lambda_j)}{\mu\ \ln(2)} - \frac{1}{\frac{g_{k,j}}{1+\sum\limits_{\substack{i\in S_k \\ i\neq j}} p_{k,i}\ g_{k,i}}}\right]^{+}, \tag{12}$$

where $[x]^+$ represents max (0, x) operation. Thus, to solve the problem in (8) using Lagrange dual decomposition, firstly $p_{k,j}$ is substituted from (12) into the Lagrangian function $L(\{\mathbf{P}\}, \boldsymbol{\lambda}, \mu)$ given in (9). Then, the Lagrangian function becomes a function of only Lagrangian multipliers, and the dual problem shown in (10) may be solved using solvers such as MATLAB's $fmincon$. This gives the optimal value of Lagrange multipliers. Substituting the values of Lagrangian multipliers in (12) gives the power allocated $p_{k,j}$ at user j and RE k. Since the optimization problem (8) is non-convex, a duality gap exists, but as the number of frequency carriers increase, it is nearly zero [39].

C. Phase Optimization

Given **F** and **P**, the original optimization problem in (6) is given as follows:

$$\mathcal{P}(\text{A3}): \quad \max_{\boldsymbol{\theta}} f_{\text{A3}}(\boldsymbol{\theta}) = \sum_{k=1}^{K}\sum_{j=1}^{J} \log_2(1+\gamma_{k,j}) \tag{13a}$$

$$\text{s.t.} \quad (6b). \tag{13b}$$

The non-convex modulus constraints in (6b) makes problem (13) difficult to solve. The search space of problem $\mathcal{P}(\text{A3})$ is the product of unit modulus circles in the complex plane, which is a Riemannian submanifold with the product geometry, and its stationary solution can be obtained using the RCG algorithm [49]. The RCG algorithm was used for precoder design [50] and for phase optimization in the IRS system [34], [35], [51]–[54]. For ease of representation, we define $\mathbf{H}^r_{k,j} = \text{diag}(\mathbf{l})\mathbf{h}^r_{k,j}$, as the effective channel for the IRS link. Thus, (2) is given as

$$\gamma_{k,j} = \frac{|h^d_{k,j} + \boldsymbol{\theta}\mathbf{H}^r_{k,j}|^2 E(x^2_{k,j})}{\sum\limits_{\substack{i\in S_k \\ i\neq j}} |h^d_{k,i} + \boldsymbol{\theta}\mathbf{H}^r_{k,j}|^2 E(x^2_{k,i}) + \sigma^2}. \tag{14}$$

A manifold $\mathcal{M}$ is a topological space in which each point's neighborhood is homeomorphic to the Euclidean space [49]. A homeomorphism is a continuous function between topological spaces that has a continuous inverse function. The examples of manifolds are line, circle, sphere, parabola, hyperbola, etc. A Riemannian manifold is a manifold whose tangent spaces are endowed with a positive-definite inner product. This characterizes the direction which produces the steepest increase at z.

In the RCG algorithm, firstly, a set of conjugate directions is generated, and then search to find the minimum value of the objective function. The problem $\mathcal{P}(\text{A3})$ can be solved using the RCG algorithm in the following three steps:

1) Compute Riemannian Gradient: The orthogonal projection of Euclidean gradient onto the tangent space is called Riemannian gradient. The Riemaninian gradient of (13a) is

$$\text{grad} f_{\text{A3}} = \Delta f_{\text{A3}} - \text{Re}\{\Delta f_{\text{A3}} \circ \boldsymbol{\theta}^*\} \circ \boldsymbol{\theta},$$

where Δf_{A} is the Euclidean gradient.

2) Search direction: The search direction can be found as the tangent vector conjugate to gradf_{A} :

$$\mathbf{d} = -\text{grad} f_{\text{A3}} + \tau \mathcal{T}(\bar{\mathbf{d}}), \tag{15}$$

where τ is the conjugate gradient update parameter, $\bar{\mathbf{d}}$ is the previous search direction, and $\mathcal{T}(\cdot)$ is the transport function given as

$$\mathcal{T}(\mathbf{d}) = \bar{d} - \text{Re}\{\mathbf{d} \circ \boldsymbol{\theta}^*\} \circ \boldsymbol{\theta},$$

3) Retraction: As a point moves alongside the tangent vector, it might not stay on the manifold. The tangent vector can be mapped back to the complex circle manifold using retraction operation as

$$\theta_n \longleftarrow \frac{(\theta + \tau_2 \mathbf{d})_n}{|(\theta + \tau_2 \mathbf{d})_n|} \tag{16}$$

where τ_2 denotes the step size obtained by Armijo backtracking line search to guarantee the objective function (13a) to be non-decreasing [49], [55].

After following the above steps in each iteration, the RCG algorithm converges for problem $\mathcal{P}(\text{A3})$ where the Riemannian Gradient will be equal to zero.

D. Complexity Analysis

The AO approach is an iterative algorithm. Each iteration involves three subproblems for solving **F**, **P**, and $\boldsymbol{\theta}$. The complexity of the Riemannian conjugate gradient (RCG) method for phase optimization is mainly dependent on computing the Euclidean gradient and retraction step [34]. The complexity of computing the Euclidean gradient is $O(J^2N^2)$, and the complexity of the retraction step is $O(J^2N)$ and can be ignored for large values of N. Further, the complexity of the power allocation algorithm is dependent on solving the dual problem. The complexity of solving the dual problem is $O(I_f(Jd_v))$, where I_f is the number of iterations required to compute the dual variables. The complexity of Algorithm 1 for factor graph matrix assignment is dependent on the number of users and on the channel conditions. In Algorithm 1, d_v REs with best channel conditions are chosen for one user, which will be indexed with value one for that user. Assuming the complexity of choosing d_v REs for each user with best channel conditions is $O(a1)$. If for another user, the indices for current d_v values do not match with any of the prior users, then the complexity will be $O(a1)$. In case the indices match, then the next highest d_v values are chosen, then the complexity increases by $O(a1)$. Every time the indexes match with any other user, the complexity increases by $O(a1)$. Thus, the overall complexity is constant value times the number of users, and so is proportional to $O(J)$. Thus, the overall complexity of the AO algorithm is $O(I_o(I_R J^2N^2 + I_f J d_v + J))$, where I_o is the number of iterations of the AO algorithm, and I_R is the number of the iterations of the RCG algorithm, respectively.

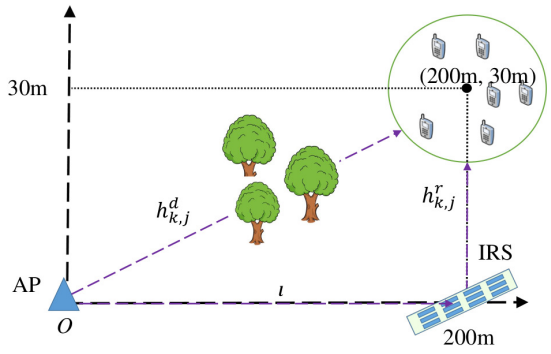

Fig. 4. Simulated IRS-assisted SCMA communication system consisting of an AP, J number of users and one N-element IRS.

IV. Results and Discussion

In this section, the performance of the proposed algorithms in Section III is evaluated. The simulation setup consists of one access point (AP) located at (0 m, 0 m), an IRS at (200 m, 0 m), and J users being served by AP and IRS, as shown in Fig. 4. The users are uniformly and randomly distributed in a circle of radius 20 m, and the center of the circle is at (200 m, 30 m). The line-of-sight (LoS) component is present for the AP-IRS channel, and the channel between user and IRS. The channel gains of both Los and NLoS are modeled using the 3GPP propagation environment [56]. The antenna gains at the receiver and transmitter are denoted as G_r and G_t, respectively. The channel gain β is given as [56] :

$$\beta(d)[dB] = G_t + G_r + \begin{cases} -28.0 - 20\log_{10}(f_c) - \\ 22\log_{10}(d/1m), & \text{if LoS} \\ -22.7 - 26\log_{10}(f_c) - \\ 36.7\log_{10}(d/1m), & \text{if NLoS} \end{cases} \tag{17}$$

where f_c represents the carrier frequency and d represents the distance. Assuming that $h^d_{k,j}$ follows the Rayleigh fading, and the IRS based channels (i.e., between AP and IRS, and between IRS and user) follow Rician fading. Thus, the channels $\mathbf{I}$ and $h^r_{k,j}$ are given as

$$\mathbf{I} = L_1 \left(\sqrt{\frac{\epsilon}{\epsilon+1}} \mathbf{a}_N(v)(\psi)^* + \sqrt{\frac{1}{\epsilon+1}} \bar{\mathbf{I}} \right), \tag{18}$$

$$h^r_{k,j} = L_2 \left(\sqrt{\frac{\epsilon}{\epsilon+1}} \mathbf{a}_N(\zeta_j) + \sqrt{\frac{1}{\epsilon+1}} h^{\bar{r}}_{k,j} \right), \tag{19}$$

where v, ψ, and ζ_j are the angular parameters, L_1 and L_2 represents the corresponding path-losses, $\mathbf{a}$ denotes the steering vector, and ϵ is the Rician factor [34]. The NLoS components are denoted as $\bar{\mathbf{I}}$ and $h^{\bar{r}}_{k,j}$. Thus, the fading variables $h^d_{k,j}, \bar{\mathbf{I}}$, and $h^{\bar{r}}_{k,j}$ are calculated in every frame. We take the Rician factor equal to 10 [34]. We compute the sum-rate of the IRS-aided SCMA system, when the factor graph matrix is fixed, power is uniformly distributed, and the IRS phase vector is randomly generated with the magnitude of one. This is considered the baseline case. The minimum rate for each user is 0.1 bps/Hz at the total transmit power of 30 dBm. Next, we analyze the performance of the proposed optimization algorithms in the simulation setup of 4×6 and 5×10 SCMA block, respectively. In case of 4×6 block, six users communicate over four REs, and thus the overloading factor is $\lambda = J/K = 6/4 = 1.5$. Similarly, in the case of 5×10 block, ten users communicate over five REs, and thus the overloading factor is $\lambda = J/K = 10/5 = 2$.

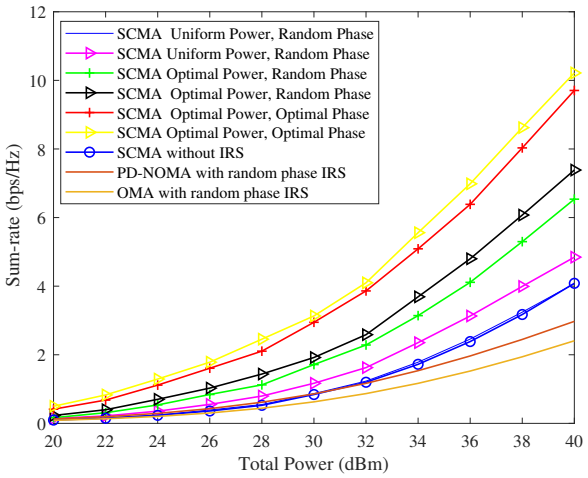

Fig. 5. Sum-rate versus transmit power for IRS-aided SCMA system with $K = 4, J = 6$ and $N = 100$, where '+' denotes the fix $\mathbf{F}$ and '▷' denotes the proposed $\mathbf{F}$ using **Algorithm 1**.

A. Sum-Rate Analysis for 4×6 SCMA Block

In this subsection, user locations are randomly generated once, and then fixed for the rest of the simulations. All the simulation curves are generated by averaging over 10^4 randomly and independently realizations of small-scale channel fading.

Fig. 5 shows the sum-rate of the proposed algorithms with respect to the total transmit power for $J = 6, K = 4$ and $N = 100$. It is to be noted that the baseline with random phase vector, fix factor graph matrix and uniform power allocation shows negligible performance gain when no IRS is deployed. Then, we have shown the effect of introducing the proposed schemes gradually. Firstly, for a uniform power and random phase vector at IRS, we optimized the factor graph matrix using **Algorithm 1**. With this, the sum-rate performance improved as compared to baseline as power increases. Next, we have shown the effect of power allocation (as shown in (12)) with random and proposed factor graph matrix and random phase vectors at IRS. Next, we optimized the phase vector using the RCG algorithm and shown the performance for random and proposed factor graph matrix, proposed power allocation and optimized phase vector of IRS. It is evident that the proposed AO scheme notably improve the sum-rate, especially as the transmit power increases. In PD-NOMA, power is allocated such that more power is allocated to the weak user under the given power

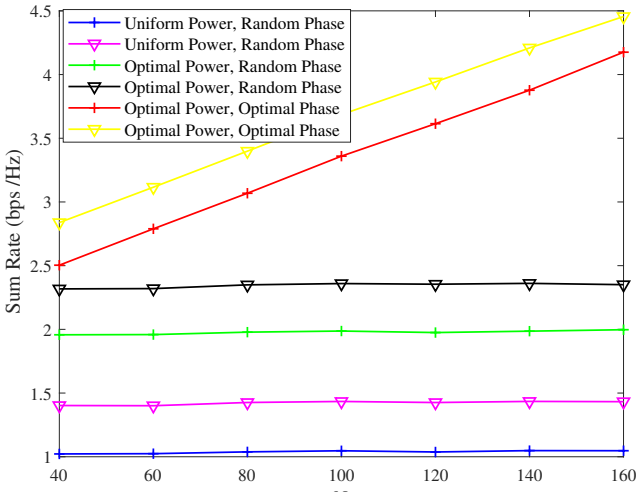

Fig. 6. Sum-rate versus N for $J = 6$ and $K = 4$ with total transmit power = 30 dBm, where '+' denotes the fix **F** and '▷' denotes the proposed **F** using **Algorithm 1**.

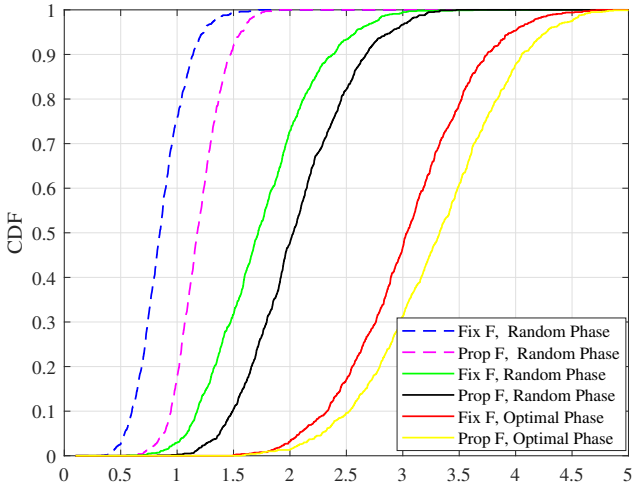

Fig. 8. CDF curves with total transmit power of 30 dBm, $J = 6, K = 4$ and $N = 100$, where dashed line represents uniform power allocation, solid line denotes optimal power allocation, 'Fix F' denotes **F** in (3), 'Prop F' denotes **F** generated from Algorithm 1.

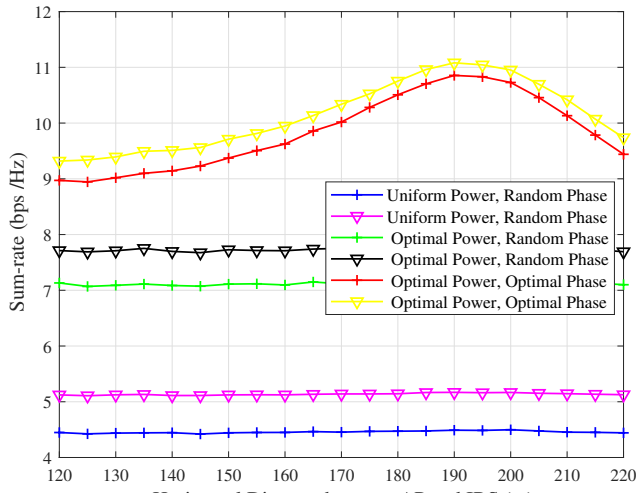

Fig. 7. Sum-rate versus the horizontal distance between IRS and AP with total transmit power of 40 dBm, $J = 6, K = 4$ and $N = 100$, where '+' denotes the fix **F** and '▷' denotes the proposed **F** using **Algorithm 1**.

budget [5]. In OMA scheme, time division multiple access (TDMA) scheme is implemented with random phases and uniform power allocation across all the users as the baseline scheme.

Fig. 6 shows the sum-rate performance with respect to N, assuming the total power is equal to 30 dBm. The sum-rate with proposed power and factor graph matrix is significantly higher than the baseline case. It is noted that when the IRS has random phase, sum-rate improvement can be seen by a small value as compared to optimized phases with increasing N.

Next, the effect of the IRS deployment on the sum-rate is shown. The horizontal distance between IRS and AP is denoted by D_{AI}. The users are generated randomly over 100 snapshots and 1000 small-scale channel realizations are generated for each snapshot. Fig. 7 illustrates the impact on the sum-rate with change in D_{AI} at $P_{tot} = 40$ dBm and $N = 100$. It is to be noted that, as D_{AI} is increased from 200 m to 220 m, the sum-rate decreases. The reason is that the combined path-loss of the IRS link $\mathbf{H}_{k,j}^{r}$ increases, as D_{AI} increases. However, when D_{AI} decreases from 200 m to 120 m, the sum-rate increases firstly but later decreases. The reason being, although the distance through IRS-assisted link decreases, the propagation conditions might not have improved. The optimal location of IRS is found to be D_{AI} = 190 m. Fig. 8 shows the cumulative distribution function (CDF) of the sum-rate corresponding to the proposed algorithms. This concludes that the sum-rate corresponding to the proposed methods improves even though the channel realizations and user locations are changed.

B. Sum-Rate Analysis for 5×10 *SCMA Block*

In this subsection, we consider the SCMA block of $K = 5, J = 10, \lambda = J/K = 2$, i.e., 10 users are concurrently transmitting data over 5 REs. An example of the factor graph matrix corresponding to 5×10 SCMA block is [57]

$$\mathbf{F}_{5\times 10} = \begin{bmatrix} 1 & 1 & 1 & 1 & 0 & 0 & 0 & 0 & 0 & 0 \\ 1 & 0 & 0 & 0 & 1 & 1 & 1 & 0 & 0 & 0 \\ 0 & 1 & 0 & 0 & 1 & 0 & 0 & 1 & 1 & 0 \\ 0 & 0 & 1 & 0 & 0 & 1 & 0 & 1 & 0 & 1 \\ 0 & 0 & 0 & 1 & 0 & 0 & 1 & 0 & 1 & 1 \end{bmatrix}. \quad (20)$$

Fig. 9 shows the sum-rate of the methods proposed in Section III with respect to the total transmit power for $J = 10, K = 5$, and $N = 100$. In this case, the total transmit power is divided among ten users, so power allotted per user is less than for $J = 6$ block, and d_f increases to 4. Similar to previous, here as well, the curves are generated by averaging

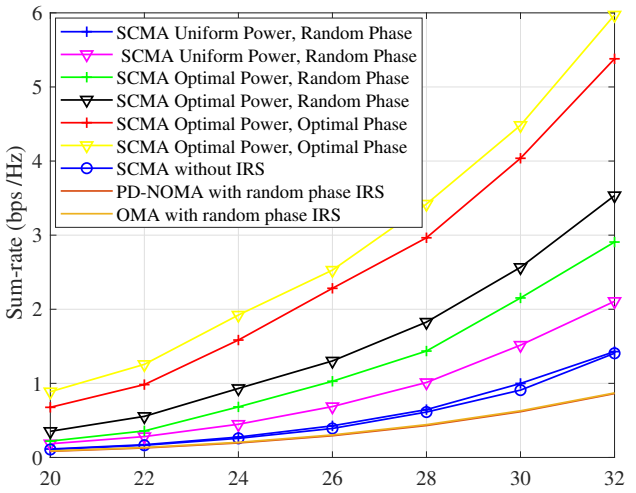

Fig. 9. Sum-rate versus total power for IRS-aided SCMA system with $J = 10, K = 5$ and $N = 100$, where '+' denotes the fix **F** and '▷' denotes the proposed **F** using **Algorithm 1**.

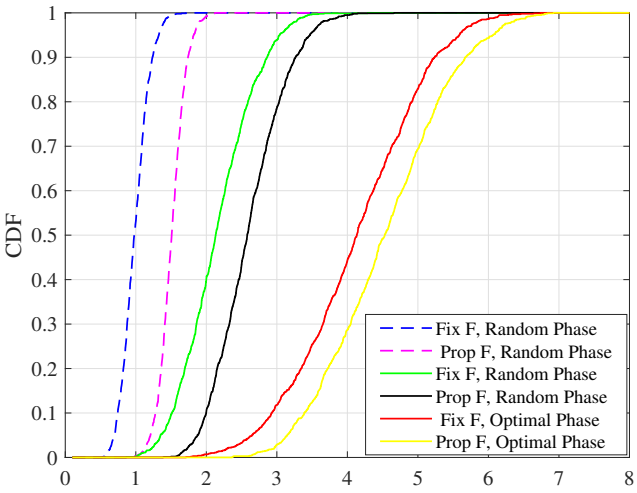

Fig. 11. CDF curves with total transmit power of 30 dBm, $J = 10, K = 5$ and $N = 100$, where dashed line represents uniform power allocation, solid line denotes optimal power allocation, 'Fix F' denotes **F** in (20), 'Prop F' denotes **F** generated from Algorithm 1.

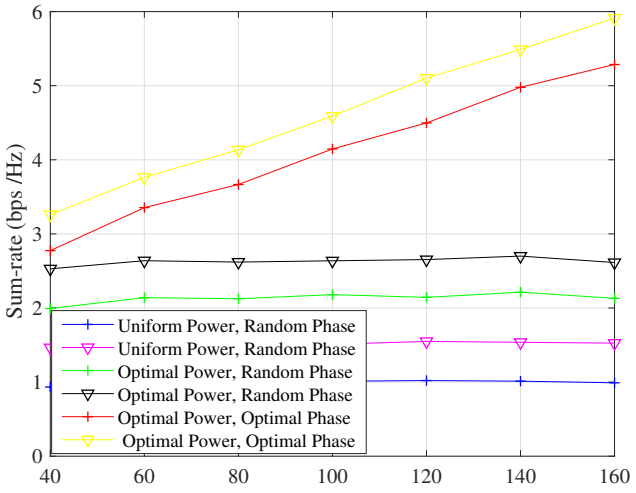

Fig. 10. Sum-rate versus N for $J = 10$ and $K = 5$ with total transmit power = 30 dBm, where '+' denotes the fix **F** and '▷' denotes the proposed **F** using **Algorithm 1**.

the sum-rate over 10^4 independent channel realizations of small-scale fading. It is to be noted that, the baseline with random phase vector, factor graph matrix and uniform power allocation shows negligible performance gain than the case when no IRS is deployed. Next, using the proposed alternate optimization scheme, the sum-rate for 5×10 SCMA block significantly improves.

Fig. 10 shows the sum-rate for 5×10 SCMA block with respect to N, assuming the total power to be 30 dBm. The sum-rate with the proposed power and factor graph matrix is significantly higher than the baseline case. However, the sum-rate does not improve with the increase in N because of the random phase vector, even with optimized power and factor graph matrix . When the IRS phase vector is optimized using the RCG algorithm, the sum-rate increases with N. Fig. 11 shows the CDF curves of the sum-rate of the proposed optimization schemes over different snapshots and channel realizations. Thus, the sum-rate of the proposed schemes perform better irrespective of the channel realizations and user locations. Table II shows the sum-rate performance of the proposed AO based algorithm for five initial iterations at the total power of 30 dBm. In each iteration, we solved three sub-problems S1 to S3, each for factor graph matrix (**F**) assignment, power allocation (**P**), and phase optimization ($\boldsymbol{\theta}$). Specifically, we have shown the effect of each proposed schemes, and the AO algorithm is terminated when the fractional increase in the sum-rate is less than 0.1%.

V. Conclusion

This work investigated the sum-rate in IRS-aided downlink SCMA system. In particular, we formulated a joint power, factor graph matrix, and IRS phase optimization problem in order to maximize the sum-rate, subject to the constraints of the SCMA CB structure, transmit power, minimum rate and IRS coefficients. The formulated problem is MINLP and hard to solve. We have proposed to solve the joint optimization problem using AO method by dividing the main problem into three sub-problems. In the first place, an algorithm based on available CSI is proposed to solve the factor graph matrix assignment sub-problem under factor graph matrix constraints. Then, for a given the factor graph matrix, we have utilized the Lagrangian dual decomposition method for power allocation. Lastly, we have optimized the IRS phase vector using RCG algorithm for maximizing the system's sum-rate. It is shown using the simulation results that the proposed algorithms outperform by optimizing the factor graph matrix, power at the BS, and phase vector of the IRS. Also, it is seen

TABLE II
PERFORMANCE OF AO ALGORITHM IN TERMS OF SUM-RATE WITH INCREASING NUMBER OF ITERATIONS.

Proposed Scheme	**Iter. 1**	**Iter. 2**	**Iter. 3**	**Iter. 4**	**Iter. 5**
S1: Initial phase, Initial power, Proposed **F**	1.14	3.17	4.02	4.037	4.043
S2: Initial phase, Lagrange based allocated power, Proposed **F**	1.92	3.964	4.028	4.041	4.044
S3: Optimized IRS phases, Lagrange based allocated power, Proposed **F**	3.17	4.02	4.037	4.043	4.045

from the results that the proposed IRS-aided SCMA system performs better than the SCMA system without the IRS.

ACKNOWLEDGMENT

The authors would like to thank the Editor Dr. Xuanyu Cao and the anonymous reviewers for their constructive suggestions which have greatly helped to improve the quality of this work. The authors are also thankful to Mr. Ashutosh Vaish and Ms. Akshita Gupta for the various discussions. Z. Liu was supported in part by the UK Engineering and Physical Sciences Research Council under Grant EP/P03456X/1 and by the Research Council of Norway under Grant 311646/070.

REFERENCES

[1] P. Yang, Y. Xiao, M. Xiao, and S. Li, "6G wireless communications: Vision and potential techniques," *IEEE Netw.*, vol. 33, no. 4, pp. 70–75, Apr. 2019.

[2] Q. Wu and R. Zhang,"Towards smart and reconfigurable environment: Intelligent reflecting surface aided wireless network," *IEEE Commun. Mag.*, vol. 58, no. 1, pp. 106–112, Jan. 2020.

[3] Z. Ding, X. Lei, G. K. Karagiannidis, R. Schober, J. Yuan, and V. K. Bhargava, "A survey on non-orthogonal multiple access for 5G networks: Research challenges and future trends," *IEEE J. Sel. Areas Commun.*, vol. 35, no. 10, pp. 2181-2195, Oct. 2017.

[4] S. Chen, Y.-C. Liang, S. Sun, S. Kang, W. Cheng, and M. Peng, "Vision, requirements, and technology trend of 6G: how to tackle the challenges of system coverage, capacity, user data-rate and movement speed," *IEEE Wireless Commun.*, vol. 27, no. 2, pp. 218-228, Apr. 2020.

[5] S. M. R. Islam, N. Avazov, O. A. Dobre, and K.-S. Kwak, "Power domain non-orthogonal multiple access (NOMA) in 5G systems: Potentials and challenges," *IEEE Commun. Surveys Tuts.*, vol. 19, no. 2, pp. 721–742, 2nd Quart., 2017.

[6] Z. Yang, Z. Ding, P. Fan, and N. Al-Dhahir, "A general power allocation scheme to guarantee quality of service in downlink and uplink NOMA systems," *IEEE Trans. Wireless Commun.*, vol. 15, no. 11, pp. 7244–7257, Nov. 2016.

[7] H. Nikopour and H. Baligh,"Sparse code multiple access," in *Proc. IEEE 24th Int. Symp. Pers. Indoor Mobile Radio Commun. (PIMRC)*, London, UK, 2013, pp. 332–336.

[8] M. Moltafet, N. M. Yamchi, M. R. Javan, and P. Azmi, "Comparison study between PD-NOMA and SCMA," *IEEE Trans.Veh. Technol.*, vol. 67, no. 2, pp. 1830–1834, Feb. 2018.

[9] Q. Luo et al., "An error rate comparison of power domain non-orthogonal multiple access and sparse code multiple access," *IEEE Open J. Commun. Soc.*, vol. 2, pp. 500–511, 2021.

[10] S. Moon, H.-S. Lee, and J.-W. Lee, "SARA: Sparse code multiple access-applied random access for IoT devices," *IEEE Internet Things J.*, vol. 5, no. 4, pp. 3160–3174, Aug. 2018.

[11] S. Chaturvedi, Z. Liu, V. A. Bohara, A. Srivastava and P. Xiao, "A Tutorial on Decoding Techniques of Sparse Code Multiple Access," *IEEE Access*, vol. 10, pp. 58503-58524, 2022.

[12] S. Han, X. Tai, W. Meng, and C. Li, "A resource scheduling scheme based on feedback for SCMA grant-free uplink transmission," in *Proc. IEEE Int. Conf. Commun. (ICC)*, Paris, France, May 2017, pp. 1–6.

[13] K. Deka, A. Thomas and S. Sharma, "OTFS-SCMA: A Code-Domain NOMA Approach for Orthogonal Time Frequency Space Modulation," in *IEEE Trans. Commun.*, vol. 69, no. 8, pp. 5043-5058, Aug. 2021.

[14] B. Lin, X. Tang, Z. Zhou, C. Lin, and Z. Ghassemlooy, "Experimental demonstration of SCMA for visible light communications," *Opt. Commun.*, vol. 419, pp. 36–40, July 2018.

[15] S. Chaturvedi, D. N. Anwar, V. A. Bohara, A. Srivastava and Z. Liu, "Low-Complexity Codebook Design for SCMA-Based Visible Light Communication," *IEEE Open J. Commun. Soc.*, vol. 3, pp. 106-118, 2022.

[16] X. Mu, Y. Liu, L. Guo, J. Lin, and N. Al-Dhahir, "Exploiting intelligent reflecting surfaces in NOMA networks: Joint beamforming optimization," *IEEE Trans. Wireless Commun.*, vol. 19, no. 10, pp. 6884–6898, Oct. 2020.

[17] X. Mu, Y. Liu, L. Guo, J. Lin, and N. Al-Dhahir, "Capacity and optimal resource allocation for IRS-assisted multi-user communication systems," *IEEE Trans. Commun.*, vol. 69, no. 6, pp. 3771–3786, June 2021.

[18] M. Fu, Y. Zhou, and Y. Shi, "Reconfigurable intelligent surface empowered downlink non-orthogonal multiple access," *IEEE Trans. Commun.*, vol. 69, no. 6, pp. 3802–3817, Jun. 2021.

[19] J. Zhu, Y. Huang, J. Wang, K. Navaie, and Z. Ding, "Power efficient IRS-assisted NOMA," *IEEE Trans. Commun.*, vol. 69, no. 2, pp. 900–913, Feb. 2021.

[20] B. Zheng, Q. Wu, and R. Zhang, "Intelligent reflecting surface-assisted multiple access with user pairing: NOMA or OMA?" *IEEE Commun. Lett.*, vol. 24, no. 4, pp. 753–757, Apr. 2020.

[21] G. Yang, X. Xu, and Y.-C. Liang, "Intelligent reflecting surface assisted non-orthogonal multiple access," in *Proc. IEEE WCNC*, Apr. 2020, pp. 1–6.

[22] J. Zuo, Y. Liu, Z. Qin, and N. Al-Dhahir, "Resource allocation in intelligent reflecting surface assisted NOMA systems," *IEEE Trans. Commun.*, vol. 68, no. 11, pp. 7170–7183, Nov. 2020.

[23] X. Mu, Y. Liu, L. Guo, J. Lin, and R. Schober, "Joint deployment and multiple access design for intelligent reflecting surface assisted networks," *IEEE Trans. Wireless Commun.*, vol. 20, no. 10, pp. 6648–6664, Oct. 2021.

[24] W. Ni, X. Liu, Y. Liu, H. Tian, and Y. Chen, "Resource allocation for multi-cell IRS-aided NOMA networks," *IEEE Trans. Wireless Commun.*, vol. 20, no. 7, pp. 4253–4268, Jul. 2021.

[25] A. S. D. Sena et al., "What role do intelligent reflecting surfaces play in multi-antenna non-orthogonal multiple access?" *IEEE Wireless Commun.*, vol. 27, no. 5, pp. 24–31, Oct. 2020.

[26] Y. Liu, Z. Qin, M. Elkashlan, Z. Ding, A. Nallanathan, and L. Hanzo, "Non-orthogonal multiple access for 5G and beyond," *Proc. IEEE*, vol. 105, no. 12, pp. 2347–2381, Dec. 2017.

[27] H. Wang, C. Liu, Z. Shi, Y. Fu and R. Song, "Power minimization for uplink RIS-assisted CoMPNOMA networks with GSIC," *IEEE Trans. Commun.*, vol. 70, no. 7, pp. 4559-4573, Jul. 2022.

[28] L. Yu, Z. Liu, M. Wen, D. Cai, S. Dang, Y. Wang, P. Xiao, "Sparse Code Multiple Access for 6G Wireless Communication Networks: Recent Advances and Future Directions," *IEEE Commun. Stand. Mag.*, vol. 5, no. 2, pp. 92-99, June 2021.

[29] I. Al-Nahhal, O. A. Dobre and E. Basar, "Reconfigurable intelligent surface-assisted uplink sparse code multiple access," *IEEE Commun. Lett.*, vol. 25, no. 6, pp. 2058-2062, June 2021.

[30] S. Sharma, K. Deka, Y. Hong and D. Dixit, "Intelligent Reflecting Surface-Assisted Uplink SCMA System," *IEEE Commun. Lett*, vol. 25, no. 8, pp. 2728-2732, Aug. 2021.

[31] I. Al-Nahhal, O. A. Dobre, E. Basar, T. M. N. Ngatched and S. Ikki, "Reconfigurable Intelligent Surface Optimization for Uplink Sparse Code Multiple Access," *IEEE Commun. Lett*, vol. 26, no. 1, pp. 133-137, Jan. 2022.

[32] G. C. Alexandropoulos and E. Vlachos, "A hardware architecture for reconfigurable intelligent surfaces with minimal active elements for

explicit channel estimation," *arXiv*, Feb. 2020. [Online]. Available: https://arxiv.org/abs/2002.10371.

[33] W. Jiang, Y. Zhang, J. Wu, W. Feng, and Y. Jin, "Intelligent reflecting surface assisted secure wireless communications with multiple-transmit and multiple-receive antennas," *IEEE Access*, vol. 8, pp. 86659–86673, May 2020.

[34] H. Guo, Y. Liang, J. Chen, and E. G. Larsson, "Weighted sumrate maximization for reconfigurable intelligent surface aided wireless networks," *IEEE Trans. Wireless Commun.*, vol. 19, no. 5, pp. 3064–3076, Feb. 2020.

[35] Y. Xiu et al., "Reconfigurable Intelligent Surfaces Aided mmWave NOMA: Joint Power Allocation, Phase Shifts, and Hybrid Beamforming Optimization," *IEEE Trans. Wireless Commun.*, vol. 20, no. 12, pp. 8393-8409, Dec. 2021.

[36] Y. Fu, L. Salan, C. W. Sung, and C. S. Chen, "Subcarrier and power allocation for the downlink of multicarrier NOMA systems," *IEEE Trans. Veh. Technol.*, vol. 67, no. 12, pp. 11 833–11 847, Dec. 2018.

[37] J. V. C. Evangelista, Z. Sattar, G. Kaddoum, and A. Chaaban, "Fairness and sum-rate maximization via joint subcarrier and power allocation in uplink SCMA transmission," *IEEE Trans. Wireless Commun.*, vol. 18, no. 12, pp. 5855–5867, Dec. 2019.

[38] M. Dabiri and H. Saeedi, "Dynamic SCMA codebook assignment methods: A comparative study," *IEEE Commun. Lett.*, vol. 22, no. 2, pp. 364–367, Feb. 2018.

[39] S. Han, Y. Huang, W. Meng, C. Li, N. Xu and D. Chen, "Optimal Power Allocation for SCMA Downlink Systems Based on Maximum Capacity," *IEEE Trans. Commun.*, vol. 67, Feb. 2019, pp. 1480–89.

[40] J. D. Griffin and G. D. Durgin, "Complete link budgets for backscatter-radio and RFID systems," *IEEE Antennas Propag. Mag.*, vol. 51, no. 2, pp. 11–25, Apr. 2009.

[41] Q. Wu and R. Zhang, "Intelligent reflecting surface enhanced wireless network via joint active and passive beamforming," *IEEE Trans. Wireless Commun.*, vol. 18, no. 11, pp. 5394–5409, Nov. 2019.

[42] R. Hoshyar, F. P. Wathan, and R. Tafazolli, "Novel low-density signature for synchronous CDMA systems over AWGN channel," *IEEE Trans. Signal Process.*, vol. 56, no. 4, pp. 1616–1626, Apr. 2008.

[43] Y. Lin, Y. Liu, Y. Siu, "Low complexity message passing algorithm for SCMA system," *IEEE Commun. Lett.*, vol. 20, issue: 12, pp. 2466-2469 Dec. 2016.

[44] A. Bayesteh, H. Nikopour, M. Taherzadeh, H. Baligh, and J. Ma, "Low complexity techniques for SCMA detection," in *Proc. IEEE Globecom Workshops*, San Diego, CA, USA, Dec. 2015, pp. 1-6.

[45] J. Hartmanis, "Computers and intractability: a guide to the theory of NP-completeness (michael r. garey and david s. johnson)," *Siam Review*, vol. 24, no. 1, p. 90, 1982.

[46] Y. Xu and W. Yin, "A block coordinate descent method for regularized multiconvex optimization with applications to nonnegative tensor factorization and completion," *SIAM J. Imag. Sci.*, vol. 6, no. 3, pp. 1758–1789, 2013.

[47] C. Huang, A. Zappone, G. C. Alexandropoulos, M. Debbah, and C. Yuen, "Reconfigurable intelligent surfaces for energy efficiency in wireless communication," *IEEE Trans. Wireless Commun.*, vol. 18, no. 8, pp. 4157–4170, 2019.

[48] S. Boyd and L. Vandenberghe, *Convex Optimization*. Cambridge, U.K.: Cambridge Univ. Press, 2004.

[49] P-A Absil, Robert Mahony, and Rodolphe Sepulchre. *Optimization algorithms on matrix manifolds*. Princeton University Press, 2009.

[50] X. Yu, J. Shen, J. Zhang, and K. B. Letaief, "Alternating minimization algorithms for hybrid precoding in millimeter wave MIMO systems," *IEEE J. Sel. Topics Signal Process.*, vol. 10, no. 3, pp. 485–500, 2016.

[51] R. Liu, H. Li, M. Li, and Q. Liu, "Symbol-level precoding design for intelligent reflecting surface assisted multi-user MIMO systems," in *Proc. Int. Conf. Wireless Commun. Signal Process.*, Oct. 2019, pp. 1–6.

[52] B. Guo, C. Sun, and M. Tao, "Two-way passive beamforming design for RIS-aided FDD communication systems," in *Proc. IEEE Wireless Commun. Netw. Conf.*, Nanjing, China, 2021, pp. 1–6.

[53] H. Dong, C. Hua, L. Liu, and W. Xu, "Towards integrated terrestrial-satellite network via intelligent reflecting surface," in *Proc. IEEE Int. Conf. Commun. (ICC)*, Montreal, QC, Canada, Jun. 2021, pp. 1–6.

[54] R. Liu, M. Li, Q. Liu, and A. L. Swindlehurst, "Joint symbol-level precoding and reflecting designs for IRS-enhanced MU-MISO systems," *IEEE Trans. Wireless Commun.*, vol. 20, no. 2, pp. 798-811, Feb. 2021.

[55] L. Armijo, "Minimization of functions having Lipschitz continuous first partial derivatives," *Pacific J. Math.*, vol. 16, no. 1, pp. 1–3, 1966.

[56] *Further advancements for E-UTRA physical layer aspects (Release 9)*. 3GPP TS 36.814, Mar. 2010.

[57] Z. Liu and L.-L. Yang, "Sparse or dense: A comparative study of code-domain NOMA systems," *IEEE Trans. Wireless Commun.*, vol. 20, no. 8, pp. 4769–4780, Aug. 2021.